Journal of Pathology
J Pathol 2016; **239:** 152–161
Published online 30 March 2016 in Wiley Online Library (wileyonlinelibrary.com) DOI: 10.1002/path.4708

ORIGINAL PAPER

VEGF-D promotes pulmonary oedema in hyperoxic acute lung injury

Teruhiko Sato,[1,2,†] Sophie Paquet-Fifield,[1] Nicole C Harris,[1,2] Sally Roufail,[1] Debra J Turner,[3] Yinan Yuan,[1] You-Fang Zhang,[1] Stephen B Fox,[1,4] Margaret L Hibbs,[2,5] Jennifer L Wilkinson-Berka,[5] Richard A Williams,[6,7] Steven A Stacker,[1,2,4] Peter D Sly[3,‡] and Marc G Achen[1,2,4,*]

[1] *Peter MacCallum Cancer Centre, East Melbourne, Victoria, Australia*
[2] *Ludwig Institute for Cancer Research, Parkville, Victoria, Australia*
[3] *Telethon Institute for Child Health Research and Centre for Child Health Research, University of Western Australia, Nedlands, Australia*
[4] *Sir Peter MacCallum Department of Oncology, University of Melbourne, Victoria, Australia*
[5] *Department of Immunology and Pathology, Monash University, Melbourne, Victoria, Australia*
[6] *Department of Pathology, University of Melbourne, Victoria, Australia*
[7] *Department of Anatomical Pathology, St Vincent's Hospital, Melbourne, Victoria, Australia*

**Correspondence to: M Achen, Peter MacCallum Cancer Centre, Locked Bag 1, A'Beckett Street, Victoria 8006, Australia. E-mail: Marc.achen@petermac.org*

†Current address: Kohnodai Hospital, National Center for Global Health and Medicine, Japan.
‡Current address: Child Health Research Centre, The University of Queensland, 62 Graham Street, South Brisbane, Queensland 4101, Australia.

Abstract

Leakage of fluid from blood vessels, leading to oedema, is a key feature of many diseases including hyperoxic acute lung injury (HALI), which can occur when patients are ventilated with high concentrations of oxygen (hyperoxia). The molecular mechanisms driving vascular leak and oedema in HALI are poorly understood. VEGF-D is a protein that promotes blood vessel leak and oedema when overexpressed in tissues, but the role of endogenous VEGF-D in pathological oedema was unknown. To address these issues, we exposed *Vegfd*-deficient mice to hyperoxia. The resulting pulmonary oedema in *Vegfd*-deficient mice was substantially reduced compared to wild-type, as was the protein content of bronchoalveolar lavage fluid, consistent with reduced vascular leak. Vegf-d and its receptor Vegfr-3 were more highly expressed in lungs of hyperoxic, versus normoxic, wild-type mice, indicating that components of the Vegf-d signalling pathway are up-regulated in hyperoxia. Importantly, VEGF-D and its receptors were co-localized on blood vessels in clinical samples of human lungs exposed to hyperoxia; hence, VEGF-D may act directly on blood vessels to promote fluid leak. Our studies show that Vegf-d promotes oedema in response to hyperoxia in mice and support the hypothesis that VEGF-D signalling promotes vascular leak in human HALI.

Keywords: hyperoxic acute lung injury; hyperoxia; pulmonary oedema; vascular leak; VEGF-D; VEGFR-2; VEGFR-3

Received 21 December 2015; Revised 7 February 2016; Accepted 17 February 2016

Conflict of interest statement: MGA and SAS are shareholders in Circadian Technologies and Ark Therapeutics, and are inventors on patents licensed to Vegenics and Ark Therapeutics. The authors have no other financial interests

Introduction

Leakage of fluid from blood vessels leading to oedema is a pathological trait central to many diseases, eg ischaemic stroke, myocardial infarction, wet age-related macular degeneration, and hyperoxic acute lung injury (HALI) [1]. HALI, which results from prolonged administration of high oxygen concentrations (≥50%) to patients with cardiac or pulmonary disease, involves damage to alveolar epithelial cells, blood vessel leak, and oedema in the lung [2–5]. Reactive oxygen species are thought to drive tissue damage in HALI [6] but molecular mechanisms promoting the vascular leak and oedema are poorly understood.

VEGF-D is an angiogenic and lymphangiogenic protein [7–10] that promotes cancer metastasis in animal models [9,11–13] and can be expressed in human tumours [14–16]. Human VEGF-D activates the endothelial cell surface receptors VEGFR-2 and VEGFR-3 [8]; mouse Vegf-d activates Vegfr-3 but is a poor ligand for Vegfr-2 [17]. VEGF-D is secreted from the cell in a full-length form that can be proteolytically processed to a mature form with enhanced bioactivity [18–20]. Notably, prolonged expression

of mature human VEGF-D in rabbit skeletal muscle and pig myocardium, driven by adenoviral delivery, promoted vascular leak and oedema [21,22], but the role of endogenous VEGF-D in oedema in human disease is unknown.

Here we use *Vegfd*-deficient mice to investigate the importance of endogenous Vegf-d for the pulmonary oedema occurring in response to hyperoxia. Our experimental findings demonstrate that Vegf-d signalling significantly contributes to this oedema. Moreover, our clinical studies involving patients exposed to hyperoxia indicate that VEGF-D may signal via its receptors on blood vascular endothelium to exacerbate pulmonary oedema in human HALI.

Materials and methods

Mice

Mice with targeted inactivation of the *Vegfd* gene ('*Vegfd*-deficient' mice; either hemizygous $Vegfd^{0/-}$ males or homozygous $Vegfd^{-/-}$ females – note that the *Vegfd* gene is located on the X chromosome [23]), on a pure C57BL/6 genetic background [24], were used for this study.

Tumour xenograft model

Eleven- to twelve-week-old female SCID/NOD mice (Animal Resources Centre, Perth, Australia) were subcutaneously injected with 293-EBNA-1 cell lines into the flank and primary tumours were photographed to assess oedema when they reached ~2500 mm^3. Two cell lines were compared: one stably transfected with an Apex-3 vector encoding a form of full-length human VEGF-D, designated VEGF-D-FULL-N-FLAG; and the control, which was stably transfected with an expression vector lacking the DNA sequence for VEGF-D [20].

Cell-based delivery of mouse VEGF-D

Dermal delivery of mouse Vegf-d was performed as previously documented [24]. Briefly, 293-EBNA-1 cells expressing mature mouse Vegf-d or the empty expression vector were embedded in Matrigel, injected subcutaneously into ears of SCID/NOD mice, and harvested after 1 week. Ear thickness was then measured with callipers; cells in the Matrigel plugs were counted; and oedema in the dermis was quantitated by measuring the proportion of unstained tissue using MetaMorph software. Cell numbers in the plugs were not significantly different between any of the study groups (data not shown). Values representing the average unstained area in the dermis were derived from three randomly chosen 800-pixel regions per mouse and are expressed as a percentage of the total area of dermis analysed.

Analyses of lung function and extravascular lung water weight

Thoracic gas volume (TGV) was measured at a transrespiratory pressure of 0 cm H_2O in a purpose-built plethysmograph as previously described [25]. Pressure–volume curves were measured during slow inflation–deflation manoeuvres [26]. Inspiration was induced by applying a controlled negative pressure to the plethysmograph and expiration was achieved by allowing the plethysmograph to equilibrate to atmospheric pressure through a resistor. Extravascular lung water weight (EVLW) was determined as previously described [27].

Hyperoxic exposure

Sensitivity to hyperoxia depends on the mouse strain [28]; hence, we conducted a pilot study involving hyperoxic exposure (95% O_2) with wild-type C57BL/6 mice for 24, 48, 60, and 72 h – the choice of these times was based on previous reports [27]. We found that 60 h was optimal based on the generation of significant pulmonary oedema, as assessed by monitoring EVLW, and viability of all mice. In contrast, exposure to hyperoxia for longer than 60 h resulted in lethality of some wild-type mice. For the experiments described in the Results section, mice were allowed to stabilize for 24 h in normoxia (after the 60-h hyperoxic exposure) prior to euthanasia. Seven- to ten-week-old hemizygous $Vegfd^{0/-}$ males and wild-type male littermates were used in these experiments. Gas composition was monitored every 4–8 h (ML 205; ADInstruments, Bella Vista, NSW, Australia) with an air-flow rate of 2.5 l/min to minimize changes in CO_2 and O_2.

Bronchoalveolar lavage fluid (BALF)

Lungs were lavaged (0.035 ml/g body weight, five times) with saline, and lavage fluid was collected as previously described [27]. Briefly, BALF samples were collected on ice, centrifuged (1500 rpm for 5 min at 4 °C), and supernatants stored at −70 °C for protein assays (Pierce® BCA™ Protein Assay Kit; Thermo Scientific, Waltham, MA, USA).

Immunohistochemistry

Immunostaining of mouse lung for Vegfr-3 was with a rat anti-mouse Vegfr-3 monoclonal antibody (clone AFL4, catalogue number 14-5988-81; eBioscience, San Diego, CA, USA). The procedure involved heat-induced antigen retrieval using Dako Target Retrieval Solution (pH 6.0), blocking of endogenous peroxidase by treatment with 3% H_2O_2 in methanol, and the use of biotinylated anti-rat secondary antibody (Dako, Glostrup, Denmark) and TSA amplification (TSA Indirect NEL 700001KT; PerkinElmer, Waltham, MA, USA) as described by the manufacturer. Immunostaining with rat anti-mouse CD31 monoclonal antibody (catalogue number 553370; BD Pharmingen, San Diego, USA) and quantitation of blood vessels were carried out as previously described [9]. Immunostaining for mouse podoplanin was with a hamster monoclonal antibody (catalogue number 10R-P155a; Fitzgerald, Acton, MA, USA) and a biotinylated anti-hamster secondary antibody (Vector Laboratories, Burlingame, CA, USA) as

for staining of mouse CD31. Human tissues were fixed in formalin and embedded in paraffin. Immunostaining for human VEGF-D was with VD1 monoclonal antibody that targets the central domain of human VEGF-D, as previously described [29], except that amplification was carried out using a Vectastain ABC Kit (Vector Laboratories). Human VEGFR-3 was detected using a mouse monoclonal antibody, 9D9F9 (catalogue number 356202; BioLegend Inc, San Diego, CA, USA): tissue sections were heated in a pressure cooker at 125 °C for 3 min in antigen retrieval buffer at pH 6.0 (Dako) and then incubated in methanol containing 3% H_2O_2 for 20 min prior to incubation with VEGFR-3 antibody (1.5 μg/ml) and detection using biotinylated secondary antibodies (Vector Laboratories) and TSA amplification (PerkinElmer). Human VEGFR-2 was detected using rabbit monoclonal antibody 55B11 from Cell Signaling Technology (Beverley, MA, USA; catalogue number 2479) that recognizes part of the cytoplasmic domain of the receptor, as described above for human VEGFR-3. Human CD31 was immunostained using a rabbit polyclonal antibody (ab28364; Abcam, Cambridge, MA, USA) with a protocol including trypsin-unmasking epitope retrieval and detection with biotinylated secondary antibodies and TSA. Human podoplanin was analysed using the D2-40 mouse monoclonal antibody (GenWay Biotech Inc, San Diego, CA, USA) as described above for human VEGFR-3, except that amplification was with an ABC Kit (Vectastain; Vector Laboratories). Images were acquired using an Olympus BX53 microscope, typically with ×40 objective lens, and a SPOT Model 34.4 1.4 MP Slider digital camera (Diagnostic Instruments Inc, Sterling Heights, MI, USA) using SPOT Advanced™ software.

Quantitative real-time PCR

Lungs were harvested after BAL and snap-frozen. Total RNA was extracted using Trizol (Invitrogen, Carlsbad, CA, USA) and a FastPrep-24™ PowerLyser (MP Biomedicals, Santa Ana, CA, USA) with ceramic spheres (MP Biomedicals). Samples were treated and analysed separately, without pooling. RNA was treated with DNAse I (Turbo DNA-free Kit; Ambion, Austin, TX, USA) prior to cDNA synthesis (High Capacity cDNA Reverse Transcriptase; Ambion). Taqman gene expression assays (Applied Biosystems, Foster City, CA, USA) for *Vegfd* (Mm00438965_m1), *Vegfr3* (Mm00433337_m1), and *Vegfc* (Mm00437310_m1) were normalized against β-actin (*Actb*, assay ID 4352933 E). Duplicate assays were performed with an ABI 7000 PCR machine (Applied Biosystems). Initial incubations were for 2 min at 50 °C and 10 min at 95 °C, followed by 45 cycles of 15 s at 95 °C and 1 min at 60 °C.

Ethics approvals

Ethics approvals for using animals were obtained from the Peter MacCallum Cancer Centre and Ludwig Institute for Cancer Research (Melbourne Branch). Ethics approval for work with human tissue was obtained from the Peter MacCallum Cancer Centre (approval number 10/16) and studies of human tissue were in accordance with guidelines of the National Health and Medical Research Council of Australia and principles expressed in the Helsinki Declaration.

Results

Exogenous VEGF-D promotes oedema in mice

Prolonged exposure to exogenous human VEGF-D promotes vascular leak and oedema in rabbit and pig muscle [21,22]. To assess the capacity of exogenous VEGF-D to promote oedema in mice, we expressed full-length human VEGF-D in a tumour xenograft based on injection of 293-EBNA-1 cell lines into the flanks of SCID/NOD mice (see the Materials and methods section) [9]. Tumours developed over 20–30 days and were matched for size. Macroscopic analysis revealed that 90% of tumours expressing VEGF-D exhibited oedema, indicated by readily visible extravasated fluid and red blood cells in and adjacent to tumours. No control tumours had macroscopically evident oedema (Figures 1A and 1B). In an alternative approach, a recombinant form of mature mouse Vegf-d was delivered into the ears of mice by subcutaneous injection of cells expressing the protein. Cells were mixed with Matrigel prior to injection to ensure that they were contained within a solid plug (Materials and methods section and Figure 1C). Ears exposed to mouse Vegf-d for 7 days were thicker and more swollen than those of controls (Figure 1C), and exhibited pronounced oedema in the epithelium and dermis of skin – the epithelial oedema was located around basal keratinocytes (Figures 1D–1F). Our findings from these approaches demonstrate that prolonged exposure to exogenous human or mouse VEGF-D promotes oedema in mice.

Lung function in *Vegfd*-deficient mice

As a prelude to testing the role of endogenous Vegf-d in oedema using a model of HALI in *Vegfd*-deficient mice, we conducted a baseline comparison by monitoring unchallenged mice for pulmonary morphology and function. *Vegfd*-deficient mice (on a pure C57BL/6 genetic background) had a normal respiration rate (Figure 2A) and were comparable in life-span (Figure 2B) and lung weight (Figure 2C) to wild-type littermate controls. There was no visual evidence of altered interstitial fluid volume in *Vegfd*-deficient mice – the lungs were not swollen or distended. The abundance of pulmonary blood vessels, monitored by staining for CD31, was not significantly different in wild-type and *Vegfd*-deficient mice (Figure 2D). There was no significant difference in extravascular lung water weight (EVLW) (Figure 2E), indicating that *Vegfd*-deficient mice have functional pulmonary lymphatics. We monitored thoracic gas volume (TGV)

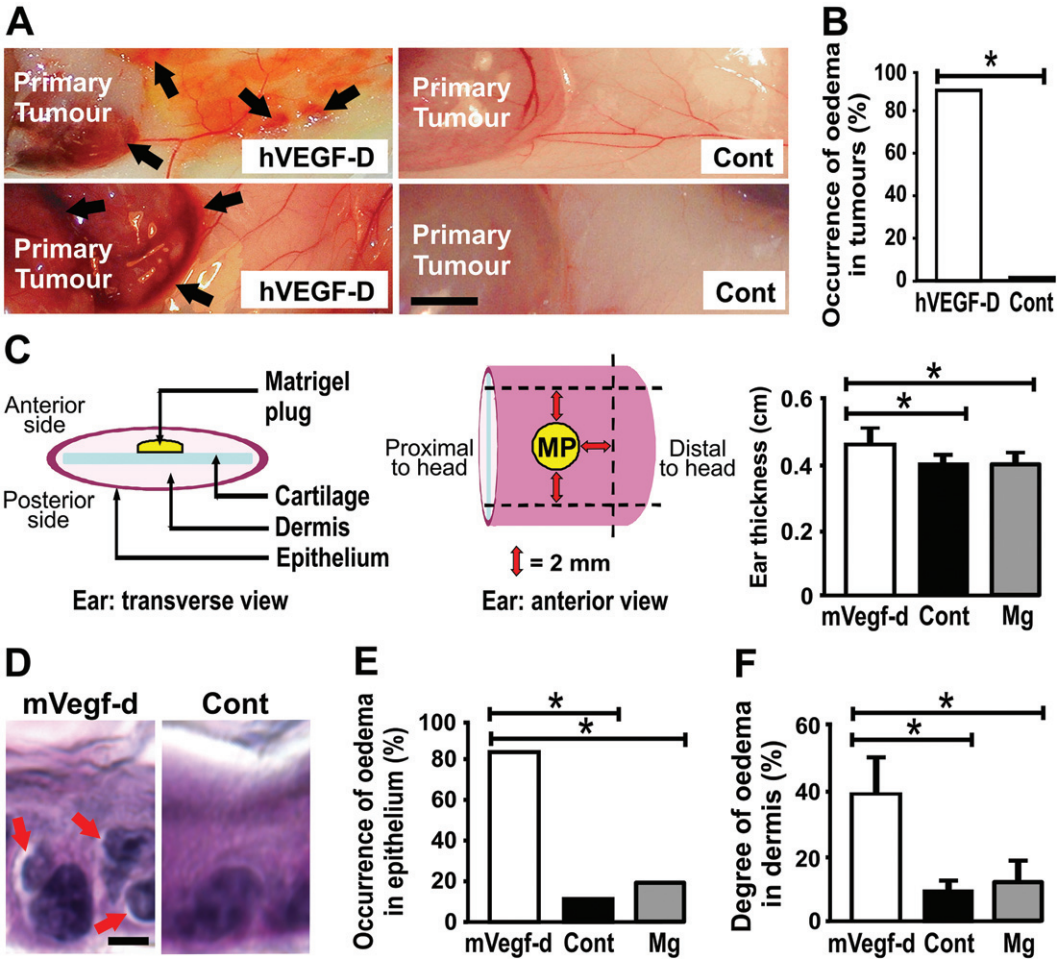

Figure 1. Exogenous VEGF-D induces oedema in mice. (A) Appearance of tumours expressing human VEGF-D (hVEGF-D) or vector lacking insert (Cont) in mouse flanks (two representative tumours from each group are shown). Note the blood vascular leak in and adjacent to tumours expressing VEGF-D (arrows). (B) Percentage of mice in which fluid accumulation was detected macroscopically. (C) Delivery model in which cells expressing mouse Vegf-d were co-injected with Matrigel into ears that were harvested 7 days later. Left: schematic diagram showing position of the Matrigel plug. Middle: schematic diagram showing positions of the callipers (dotted lines) for measuring ear thickness. Right: quantitation of ear thickness (mean ± SEM). MP = Matrigel plug; mVegf-d = cells expressing mature mouse Vegf-d; Cont = cells harbouring vector lacking *Vegfd* insert; Mg = Matrigel without cells. (D) H&E of ear epithelium after exposure to cells. Red arrows indicate pericellular oedema around basal keratinocytes. (E) Percentage of mice in which pericellular oedema was observed. (F) Quantification of oedema in dermis expressed as % dermis unstained by H&E (mean ± SEM). Data in B, C, E, and F are from two experiments. In B, $n = 10$ for both groups. In E and F, $n = 6$ for mVegf-d, $n = 9$ for Cont, $n = 5$ for Mg; and for C, $n = 10$, 8 and 5, respectively. $^*p < 0.05$ (Fisher's exact test in B and E; Student's t-test in C; Tukey's multiple comparison test in F). Scale bars in A and D = 500 and 10 µm, respectively.

using a plethysmograph to assess lung function, which revealed no difference in the TGV between wild-type and *Vegfd*-deficient mice – the pressure–volume curves were almost identical (Figure 2F). Hence, lungs of wild-type and *Vegfd*-deficient mice were similar in gross morphology and respiratory function.

Response of mice to hyperoxia

Wild-type and *Vegfd*-deficient mice were subjected to hyperoxia (95% O_2 for 60 h, see the Materials and methods section) to assess the role of endogenous Vegf-d in vascular leak and oedema occurring in response to this insult. Macroscopic observation to monitor tissue swelling and haemorrhage (Figure 3A, top panels) revealed that pulmonary oedema occurred in significantly more wild-type than *Vegfd*-deficient mice: 15 of 21 wild-type mice exhibited pulmonary oedema compared with only 4 of 17 *Vegfd*-deficient mice ($p = 0.0081$, Fisher's exact test). Wild-type mice with pulmonary oedema had pronounced intra-alveolar oedema fluid, intra-alveolar haemorrhage, and vascular congestion in the alveolar wall (Figure 3A, lower-left panel). The EVLW of *Vegfd*-deficient mice exposed to hyperoxia was significantly lower than that of wild-type mice (Figure 3B), confirming that the lungs of wild-type mice were more oedematous. We observed a significantly higher total protein concentration in the bronchoalveolar lavage fluid (BALF) of wild-type mice exposed to hyperoxia (Figure 3B), which is consistent with the finding of more severe oedema, given that the excess fluid is derived from protein-rich blood. Our findings demonstrate that Vegf-d promotes oedema in mouse lung in response to hyperoxia.

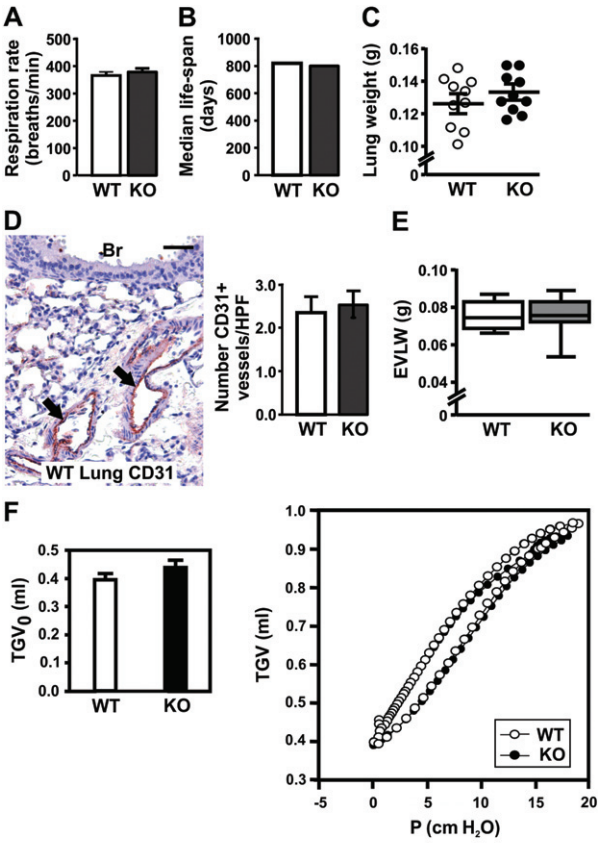

Figure 2. Comparison of lungs from unchallenged wild-type (WT) and *Vegfd*-deficient (KO) mice. Comparison of respiration rate (A), median life-span (B), lung weight (C), abundance of CD31-positive blood vessels (D), and EVLW (E). In D, the left panel shows immunostaining of WT for CD31 (arrows indicate positively stained blood vessels; Br = bronchiole); the right panel shows quantitation of CD31-positive vessels (HPF = high-power field). (F) Thoracic gas volume (TGV) measured at 0 cm H_2O transrespiratory pressure (left). Representative pressure–volume curves from a wild-type (WT) and a *Vegfd*-deficient mouse (KO) (right). Data for all panels (except left panel D and right panel F) are from two experiments. For A, $n = 15$ for WT and KO; for B, $n = 21$ for WT and 25 for KO; for C, E, and F (left), $n = 10$ for WT and KO; for D (right), $n = 5$ for WT and KO. Graphs in A, C, D, and F (left) show mean ± SEM. Graph in E shows mean, 10th to 90th percentile, maxima, and minima values. Scale bar in D = 100 µm. Data in A, C, D, E, and F (left) were compared using Student's *t*-test and in B with the Gehan–Breslow–Wilcoxon test; there were no statistically significant differences.

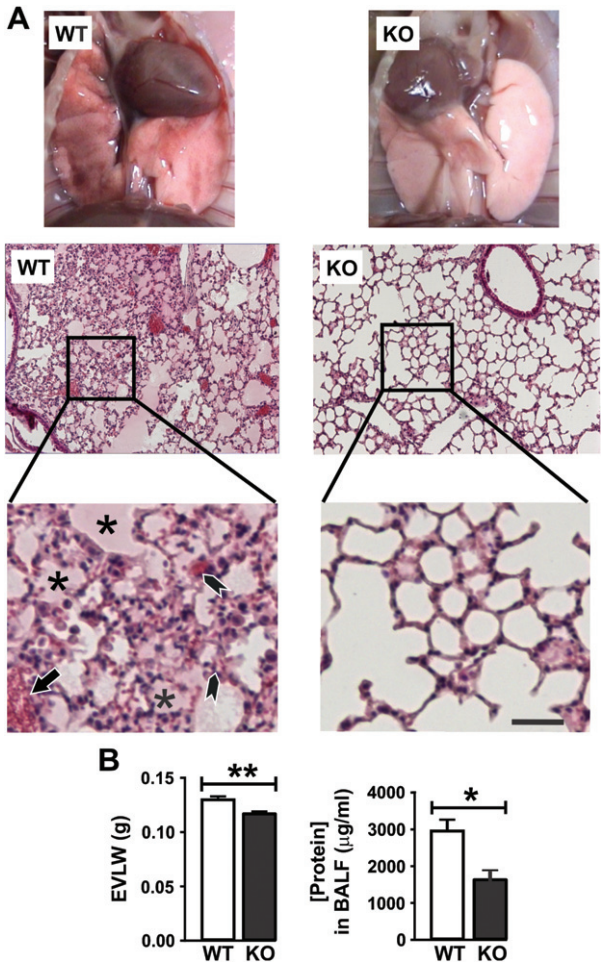

Figure 3. Effects of hyperoxia in mouse lung. (A) Representative examples of wild-type (WT) and *Vegfd*-deficient (KO) lungs after hyperoxia. *Intra-alveolar regions with proteinaceous oedema fluid; arrow, intra-alveolar haemorrhage; arrowheads, vascular congestion in alveolar wall. Scale bar = 100 µm. (B) EVLW after hyperoxia ($n = 20$ for WT; $n = 17$ for KO) and protein concentration in BALF after hyperoxia ($n = 7$ for WT and KO). $^{**}p < 0.01$; $^{*}p < 0.05$, unpaired *t*-test. Data are mean ± SEM from two experiments.

Vegf-d and Vegfr-3 in mouse lung

We monitored Vegf-d and its receptor in mouse, Vegfr-3, to assess if their expression is altered by hyperoxia and if Vegf-d might act directly on blood vessels to promote vascular leak and oedema. Quantitative RT-PCR (qRT-PCR) showed that transcripts for Vegf-d and Vegfr-3 were more abundant in wild-type lungs exposed to hyperoxia than in normoxia (Figure 4A). *Vegfr3* mRNA was also increased in hyperoxic, versus normoxic, *Vegfd*-deficient lungs. The increase in transcripts for Vegf-d and Vegfr-3 in hyperoxic wild-type lungs indicates that Vegf-d signalling may be more pronounced in hyperoxia, and may explain why EVLW is increased in wild-type versus *Vegfd*-deficient lungs under hyperoxic conditions, but not in normoxia. Transcript levels for Vegf-c, an angiogenic and lymphangiogenic growth factor that is highly structurally related to Vegf-d [30], were also up-regulated in wild-type as well as *Vegfd*-deficient mice after hyperoxic exposure (Figure 4A). However, there was no statistically significant difference between *Vegfc* mRNA levels in the lungs of *Vegfd*-deficient and wild-type mice after hyperoxic exposure.

Immunohistochemistry revealed Vegfr-3 on the endothelium of blood vessels in wild-type and *Vegfd*-deficient mice after hyperoxia (Figures 4B–4E). Vegfr-3-positive blood vessels (that were positive for CD31 and negative for the lymphatic marker podoplanin in serial sections) were more abundant in wild-type hyperoxic lung than in wild-type normoxic lung (Vegfr-3-positive blood vessels were detected in 83% of high-power fields for hyperoxic wild-type lung versus 36% for normoxic wild-type lung; $p < 0.05$, Fisher's exact test, $n = 11$ and 12 for hyperoxic and

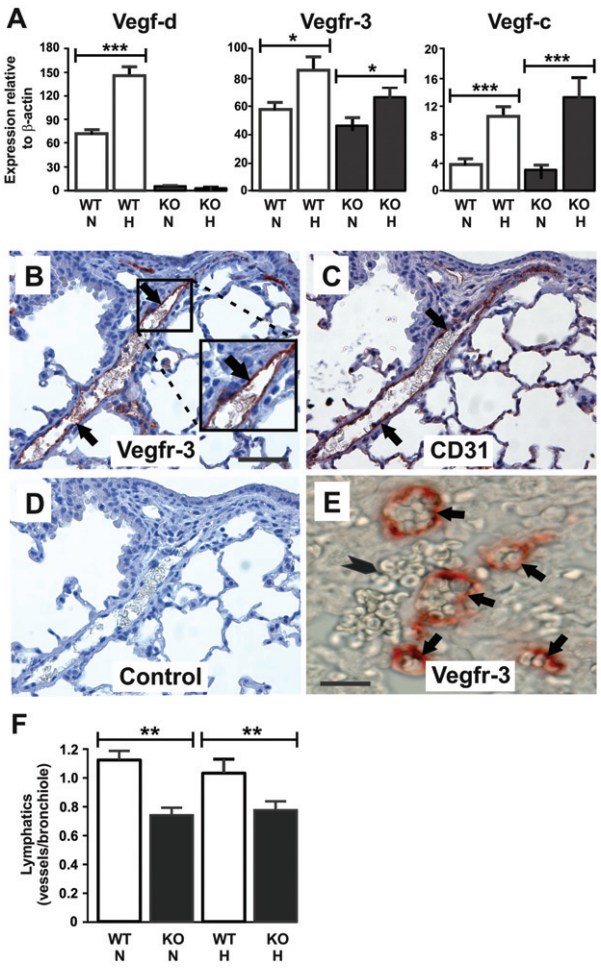

Figure 4. Vegf-d, Vegfr-3, and lymphatic vessels in mouse lung. (A) *Vegf-d*, *Vegfr-3*, and *Vegf-c* mRNA in lungs assessed by qRT-PCR (mean ± SEM). N = normoxia; H = hyperoxia. Data are from two experiments; $n = 6$ for all groups. $^{***}p < 0.001$; $^{*}p < 0.05$, unpaired *t*-test. Immunostaining of hyperoxic WT lung for Vegfr-3 (B) and, on serial section, for CD31 (C). Arrows indicate positive signals on the endothelium of the same blood vessel. (D) Negative control for B in which the primary antibody was omitted. (E) Staining of hyperoxic WT lung reveals Vegfr-3-positive blood vessels (arrows) (note erythrocytes in vessels; vessels were strongly stained for CD31 but negative for lymphatic marker podoplanin in serial sections – not shown) clustered around a region of erythrocyte leakage (arrowhead) (this region was not surrounded by blood vascular endothelium as shown by lack of CD31 staining on serial section – not shown). Scale bars in B and E = 100 and 20 μm, respectively. (F) Abundance of lymphatic vessels in lungs of WT and KO mice under normoxic conditions (N) and after hyperoxic exposure (H). Data show mean ± SEM. $n = 7$ for WT normoxic; $n = 9$ for KO normoxic; and $n = 8$ for both WT and KO hyperoxic. $^{**}p < 0.01$, Student's *t*-test. There were no significant changes in the abundance of lymphatics in *Vegfd*-deficient or wild-type mice after hyperoxia, compared with the respective non-challenged controls ($p = 0.42$ and $p = 0.32$, respectively; Student's *t*-test).

normoxic, respectively). Further, we observed clusters of Vegfr-3-positive blood vessels adjacent to regions where erythrocytes had leaked into alveoli in wild-type mice under hyperoxic conditions (Figure 4E). We also detected Vegfr-3 on lymphatic vessels (which were positively stained for podoplanin in serial section) in normoxic and hyperoxic lungs of wild-type and *Vegfd*-deficient mice – Vegfr-3 localization on lymphatics was expected as it is known to be expressed on these vessels in adult tissues [31,32]. While there were fewer pulmonary lymphatics in non-challenged *Vegfd*-deficient compared with wild-type mice, this difference did not change after hyperoxic exposure (Figure 4F). Indeed, there were no significant changes in the abundance of lymphatics in *Vegfd*-deficient or wild-type mice after hyperoxia, compared with the respective non-challenged controls. Our findings are consistent with the hypothesis that Vegf-d signalling in blood vessels is more pronounced in hyperoxia and could contribute to vascular leak and oedema in response to hyperoxia.

VEGF-D and receptors in human lung

We examined the localization of VEGF-D in patients who were retrospectively identified as having been exposed to hyperoxia before death, in order to assess the clinical relevance of our findings in mice. As human VEGF-D activates VEGFR-2 and VEGFR-3 [8], we also analysed these receptors. Given that autopsies are not often conducted on patients who die while on hyperoxic therapy, we searched the pathology departments of three local hospitals for relevant tissue. We accessed lung from a patient who died 12 h after hyperoxic therapy (patient 1) and from another who died immediately after hyperoxia (patient 2) (Figure 5A). For patient 2, we also accessed lung before hyperoxic therapy, allowing us to compare normoxic with hyperoxia-exposed lung from the same person, which to our knowledge is the first time this has been done.

Patient 1 was a male with rheumatoid arthritis and Hodgkin's lymphoma who was ventilated with O_2-enriched air (O_2 varying between 50% and 88%) over 7 days – he died 12 h after withdrawal of hyperoxia treatment (Figure 5A). Haematoxylin and eosin (H&E) staining showed abundant intra-alveolar proteinaceous oedema fluid, intra-alveolar haemorrhage, and vascular congestion in the alveolar wall (Figure 5B). Immunostaining for VEGF-D showed localization on the endothelium of many blood vessels (Figure 5C), the luminal side of bronchial epithelial cells, and pneumocytes lining alveoli (Figures 6A and 6B). The VEGF-D-positive endothelium of blood vessels was also positive for VEGFR-3 and CD31 (Figures 5E–5G). VEGFR-3 was also detected on the endothelium of lymphatic vessels (which were positively stained for podoplanin) as expected, and on pneumocytes (data not shown). VEGFR-2 was expressed on the endothelium of many blood vessels (Figure 5H) and was often co-localized with VEGF-D and VEGFR-3 on these vessels, as assessed on serial sections. Strong staining for VEGFR-2 was also detected on pneumocytes (Figure 6C).

Patient 2 was a male with a metastatic non-seminomatous germ cell tumour who underwent surgery to remove metastases. The microscopic anatomy of the normoxic lung removed at surgery, distant from any

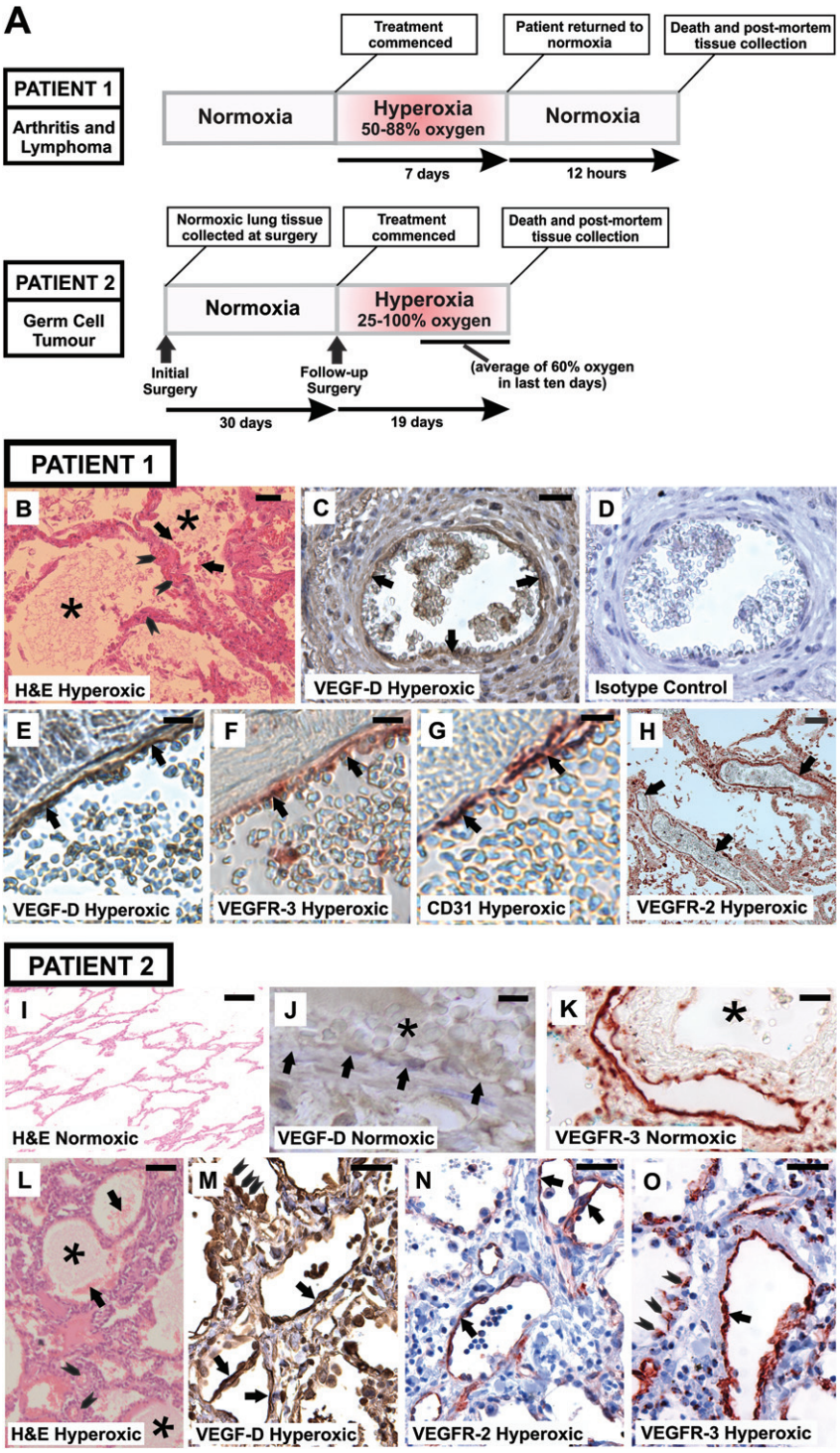

Figure 5. VEGF-D and receptors in clinical samples of hyperoxic lung. (A) Timelines for hyperoxic treatment of patients 1 and 2 (not to scale). (B–H) Analysis of patient 1 who died 12 h after withdrawal of hyperoxic therapy. (B) H&E of lung. *Intra-alveolar regions with proteinaceous oedema fluid; arrows, intra-alveolar haemorrhage; arrowheads, vascular congestion in alveolar wall. (C) Blood vessel immunostained for VEGF-D. Arrows, signal on endothelium. (D) Isotype- and concentration-matched control for VEGF-D, on section serial to C. (E) High-power image of blood vascular endothelium stained for VEGF-D. (F) Section serial to E, stained for VEGFR-3. (G) Section serial to F, stained for CD31. Arrows, signals on endothelium of the same blood vessel. (H) VEGFR-2 staining showing signal on endothelium of blood vessels (arrows). (I–O) Analysis of patient 2 who died upon withdrawal of hyperoxic therapy. (I) H&E of normoxic lung (prior to hyperoxia) – tissue is relatively normal. (J) Staining of normoxic lung for VEGF-D – a blood vessel lacking significant staining is shown (arrows, endothelium; *lumen containing abundant red blood cells). (K) Staining of normoxic lung for VEGFR-3 showing strong signal on endothelium of lymphatic vessel (this vessel was positively stained for podoplanin in serial section – not shown) but not on blood vessel (*lumen of blood vessel; this vessel was negative for podoplanin in serial section – not shown). (L) H&E after hyperoxia. *Intra-alveolar regions with proteinaceous oedema fluid; arrows, intra-alveolar haemorrhage; arrowheads, vascular congestion in alveolar wall. (M) Staining for VEGF-D after hyperoxia. Arrows, signal on endothelium of blood vessels (these vessels were negative for podoplanin in serial section – not shown); arrowheads, positively stained, swollen pneumocytes. (N) Immunostaining for VEGFR-2 on section serial to M. Arrows, signals on endothelium of blood vessels. (O) Immunostaining for VEGFR-3. Arrow, signal on endothelium of blood vessel; arrowheads, swollen, positively stained pneumocytes. Scale bar = 100 μm (B and L); 25 μm (C, H, K, M, and N); 12.5 μm (E–G, J, and O); 200 μm (I).

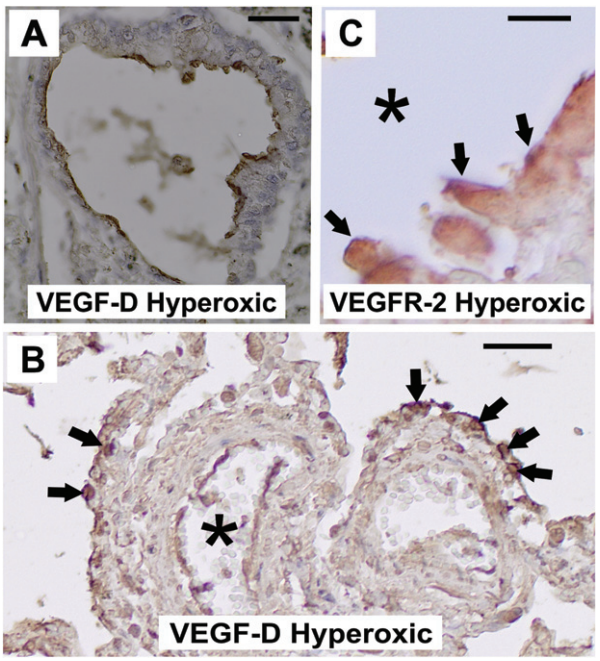

Figure 6. Immunostaining of bronchial epithelial cells and pneumocytes in hyperoxic lung tissue from patient 1. (A) VEGF-D staining showing positive signal on the luminal side of bronchial epithelial cells. (B) VEGF-D staining on pneumocytes. Arrows, signals on swollen pneumocytes lining alveoli; *lumen of blood vessel which has positively stained endothelium. (C) Immunostaining for VEGFR-2. Arrows, swollen VEGFR-2-positive pneumocytes; *lumen of alveolus. Scale bar = 10 μm (A); 100 μm (B); 5 μm (C).

tumour, was relatively normal (Figure 5I). Immunostaining for VEGF-D indicated that there was no signal on the endothelium of most blood vessels (Figure 5J). Staining for VEGFR-3 was strong on the endothelium of lymphatics but was absent or extremely weak on blood vessels (Figure 5K). In contrast, VEGFR-2 was detected on many blood vessels (similar to VEGFR-2 in patient 1; Figure 5H). Both VEGFR-2 and VEGFR-3 were also detected on pneumocytes (similar to VEGFR-2 in patient 1; Figure 6C). One month later, he underwent another operation to remove metastases from the lung. Postoperatively (day 1), he became hypoxic and was intubated. He was ventilated with O_2-enriched air (O_2 varying from 25% to 100% with an average of about 60% for the final 10 days), but died when treatment was withdrawn 19 days later. Samples of lung collected post-mortem had undergone profound change compared with his normoxic lung collected previously, with marked vascular congestion, swelling of pneumocytes, severe intra-alveolar haemorrhage, and intra-alveolar oedema fluid (Figure 5L). This hyperoxic tissue was more strongly stained for VEGF-D than normoxic lung, including staining on blood vessel endothelium and pneumocytes (Figure 5M). VEGFR-2 was also detected on the endothelium of many blood vessels (Figure 5N) and pneumocytes, often co-localized with VEGF-D. Notably, VEGFR-3 was detected on the endothelium of numerous blood vessels (Figure 5O).

Overall, these data indicate that expression of the cell surface receptors VEGFR-2 and VEGFR-3 can be up-regulated on the endothelium of blood vessels in the lungs of patients exposed to hyperoxia. These vessels also stain for VEGF-D, which could be due to receptor-mediated uptake of this growth factor. These findings are consistent with the hypothesis that the VEGF-D signalling pathway may contribute to vascular leak and oedema in HALI in the clinical setting.

Discussion

A previously unappreciated role for VEGF-D in pathological oedema has been revealed in this study using animal models of acute lung injury driven by hyperoxia as well as samples from patients exposed to hyperoxia before death. Our analyses demonstrate that the two patients studied here had key features of hyperoxic damage, including intra-alveolar haemorrhage, intra-alveolar oedema, and vascular congestion, which were similar to changes in wild-type mice exposed to hyperoxia (cf Figures 5B, 5L, and 3A), and showed co-localization of VEGF-D with VEGFR-2 and VEGFR-3 on blood vascular endothelium and pneumocytes. Notably for patient 2, staining for VEGF-D and VEGFR-3 was stronger on blood vascular endothelium in hyperoxic lung than in normoxia, and likewise, Vegfr-3-positive blood vessels were more abundant in hyperoxic mouse lung than in normoxia, altogether indicating up-regulation of multiple components of the VEGF-D signalling system associated with blood vessels. These findings are consistent with the hypothesis that VEGF-D-driven signalling in blood vessels contributes to vascular leak and oedema in HALI. Our findings also suggest that VEGF-D signalling via VEGFR-2 and/or VEGFR-3 on pneumocytes could play a role in HALI. The relative contribution of VEGFR-2 and VEGFR-3 in this condition remains to be addressed, and is complicated by potential involvement of VEGFR-2/VEGFR-3 heterodimers [33], but could be tested with neutralizing antibodies targeting these receptors in animal models of HALI.

We observed profound differences in the pulmonary blood vessels of *Vegfd*-deficient versus wild-type mice after hyperoxic exposure. Importantly, congestion of blood vessels and intra-alveolar haemorrhage were much more extensive in wild-type mice than in *Vegfd*-deficient mice after hyperoxic exposure, which was also the case for hyperoxic human lung versus normoxic lung, findings that are consistent with a key role for the leakage of blood vessels in driving the enhanced lung oedema. This is, in turn, consistent with our findings that VEGF-D can promote leakage from blood vessels in mice, as demonstrated by the extravasation of red blood cells in the 293-EBNA-1 xenograft model. Similarly, VEGF-D has been reported to increase the permeability of blood vessels and subsequent oedema in adenoviral gene delivery studies involving larger animal species [21,22]. In addition to its effects on blood vessels, VEGF-D has been shown to promote

lymphangiogenesis in animal models of disease (see ref 13 for review). Hence, it is possible that altered lymphatic vascular function in *Vegfd*-deficient mice contributed to the reduced pulmonary oedema observed in their lungs after hyperoxic exposure, compared with wild-type mice. Indeed, there are fewer pulmonary lymphatics in unchallenged *Vegfd*-deficient compared with wild-type mice and this did not alter after hyperoxic exposure [34]. Notably, lymphangiogenesis did not occur in either *Vegfd*-deficient or wild-type lungs during hyperoxic exposure. The degree to which the reduced abundance of lymphatics in *Vegfd*-deficient mice might have contributed to the less extensive oedema in the setting of hyperoxia requires further investigation.

The question arises as to whether the induction of VEGF-D by hyperoxia, leading to oedema, is simply a pathological response to oxygen therapy or has a broader biological significance. By way of comparison, hypoxia is a normal feature of ocular development and the up-regulation of VEGF-A production by hypoxia is important for regulating angiogenesis in the developing eye, as well as for a variety of disease processes [35,36]. However, we are not aware of normal developmental or common disease scenarios in which human tissues encounter pronounced hyperoxia. This indicates that the hyperoxic induction of VEGF-D production may not have a broader biological role. Nonetheless, it is conceivable, perhaps likely, that VEGF-D-mediated oedema could be induced by other triggers that do play roles in more common biological or disease settings.

It is noteworthy that levels of *Vegfc* mRNA increased in lungs of *Vegfd*-deficient mice in response to hyperoxic exposure, similar to lungs of wild-type mice. Given the functional similarities of VEGF-C and VEGF-D [8,30], the increase in *Vegfc* mRNA might have been expected to lead to functional compensation for the absence of Vegf-d in *Vegfd*-deficient mice. However, this was not the case, given the different responses of *Vegfd*-deficient and wild-type mice to hyperoxic exposure. Potential explanations for this finding include the following: (i) the increased *Vegfc* mRNA levels in the hyperoxic setting may not lead to higher Vegf-c protein levels, due to post-transcriptional regulation; (ii) there may be far more Vegf-d present in hyperoxic wild-type lung than Vegf-c, such that Vegf-c cannot functionally compensate when Vegf-d is absent; and (iii) Vegf-c and Vegf-d may have functional distinctions in terms of driving vascular leak and oedema in the hyperoxic lung.

In summary, our findings indicate that signalling by VEGF-D may contribute to vascular leak and oedema in HALI. It has been reported that another angiogenic growth factor, angiopoietin 2 (Ang2), can also promote aspects of HALI pathogenesis including inflammation and epithelial necrosis [5]. Hence, it may be possible to treat or prevent HALI by targeting signalling by these proteins. This approach could be relevant for patients with severe acute respiratory distress syndrome who require hyperoxic therapy and are at risk of HALI [6]. Investigation of the molecular mechanisms up-regulating levels of VEGF-D and Ang2 in hyperoxia may reveal other signalling pathways therapeutically relevant in HALI. Analysis of the functional significance of signalling by these proteins for the vascular leak and oedema, which are important features of other problematic diseases including ischaemic stroke, myocardial infarction, and wet age-related macular degeneration, is also warranted.

Acknowledgments

This work was supported by grants and fellowships from the National Health and Medical Research Council of Australia (to MGA, SAS, SBF, JLW-B, and MLH) and the Operational Infrastructure Support Program of the Victorian Government.

Author contribution statement

TS, SP-F, SAS, PDS, RAW, NCH, and MGA contributed to study design, data collection, data interpretation, writing of the manuscript, and revision of the manuscript. MLH, SBF, and JLW-B contributed to study design, data interpretation, and revision of the manuscript. SR, DJT, YY, and Y-FZ contributed to data collection, data interpretation, and revision of the manuscript.

References

1. Weis SM. Vascular permeability in cardiovascular disease and cancer. *Curr Opin Hematol* 2008; **15:** 243–249.
2. Barazzone C, Horowitz S, Donati YR, et al. Oxygen toxicity in mouse lung: pathways to cell death. *Am J Respir Cell Mol Biol* 1998; **19:** 573–581.
3. Crapo JD. Morphologic changes in pulmonary oxygen toxicity. *Annu Rev Physiol* 1986; **48:** 721–731.
4. Mantell LL, Horowitz S, Davis JM, et al. Hyperoxia-induced cell death in the lung –the correlation of apoptosis, necrosis, and inflammation. *Ann N Y Acad Sci* 1999; **887:** 171–180.
5. Bhandari V, Choo-Wing R, Lee CG, et al. Hyperoxia causes angiopoietin 2-mediated acute lung injury and necrotic cell death. *Nature Med* 2006; **12:** 1286–1293.
6. Kallet RH, Matthay MA. Hyperoxic acute lung injury. *Respir Care* 2013; **58:** 123–141.
7. Zheng W, Aspelund A, Alitalo K. Lymphangiogenic factors, mechanisms, and applications. *J Clin Invest* 2014; **124:** 878–887.
8. Achen MG, Jeltsch M, Kukk E, et al. Vascular endothelial growth factor D (VEGF-D) is a ligand for the tyrosine kinases VEGF receptor 2 (Flk1) and VEGF receptor 3 (Flt4). *Proc Natl Acad Sci U S A* 1998; **95:** 548–553.
9. Stacker SA, Caesar C, Baldwin ME, et al. VEGF-D promotes the metastatic spread of tumor cells via the lymphatics. *Nature Med* 2001; **7:** 186–191.
10. Wise LM, Ueda N, Dryden NH, et al. Viral vascular endothelial growth factors vary extensively in amino acid sequence, receptor-binding specificities, and the ability to induce vascular permeability yet are uniformly active mitogens. *J Biol Chem* 2003; **278:** 38004–38014.
11. Achen MG, Stacker SA. Vascular endothelial growth factor-D: signaling mechanisms, biology and clinical relevance. *Growth Factors* 2012; **30:** 283–296.

12. Karnezis T, Shayan R, Caesar C, et al. VEGF-D promotes tumor metastasis by regulating prostaglandins produced by the collecting lymphatic endothelium. *Cancer Cell* 2012; **21:** 181–195.
13. Stacker SA, Williams SP, Karnezis T, et al. Lymphangiogenesis and lymphatic vessel remodelling in cancer. *Nature Rev Cancer* 2014; **14:** 159–172.
14. Debinski W, Slagle-Webb B, Achen MG, et al. VEGF-D is an X-linked/AP-1 regulated putative onco-angiogen in human glioblastoma multiforme. *Mol Med* 2001; **7:** 598–608.
15. Stacker SA, Williams RA, Achen MG. Lymphangiogenic growth factors as markers of tumor metastasis. *APMIS* 2004; **112:** 539–549.
16. Saharinen P, Eklund L, Pulkki K, et al. VEGF and angiopoietin signaling in tumor angiogenesis and metastasis. *Trends Mol Med* 2011; **17:** 347–362.
17. Baldwin ME, Catimel B, Nice EC, et al. The specificity of receptor binding by vascular endothelial growth factor-D is different in mouse and man. *J Biol Chem* 2001; **276:** 19166–19171.
18. Baldwin ME, Roufail S, Halford MM, et al. Multiple forms of mouse vascular endothelial growth factor-D are generated by RNA splicing and proteolysis. *J Biol Chem* 2001; **276:** 44307–44314.
19. Harris NC, Paavonen K, Davydova N, et al. Proteolytic processing of vascular endothelial growth factor-D is essential for its capacity to promote the growth and spread of cancer. *FASEB J* 2011; **25:** 2615–2625.
20. Stacker SA, Stenvers K, Caesar C, et al. Biosynthesis of vascular endothelial growth factor-D involves proteolytic processing which generates non-covalent homodimers. *J Biol Chem* 1999; **274:** 32127–32136.
21. Rissanen TT, Markkanen JE, Gruchala M, et al. VEGF-D is the strongest angiogenic and lymphangiogenic effector among VEGFs delivered into skeletal muscle via adenoviruses. *Circ Res* 2003; **92:** 1098–1106.
22. Rutanen J, Rissanen TT, Markkanen JE, et al. Adenoviral catheter-mediated intramyocardial gene transfer using the mature form of vascular endothelial growth factor-D induces transmural angiogenesis in porcine heart. *Circulation* 2004; **109:** 1029–1035.
23. Jenkins NA, Woollatt E, Crawford J, et al. Mapping of the gene for vascular endothelial growth factor-D in mouse and man to the X chromosome. *Chromosome Res* 1997; **5:** 502–505.
24. Paquet-Fifield S, Levy SM, Sato T, et al. Vascular endothelial growth factor-d modulates caliber and function of initial lymphatics in the dermis. *J Invest Dermatol* 2013; **133:** 2074–2084.
25. Janosi TZ, Adamicza A, Zosky GR, et al. Plethysmographic estimation of thoracic gas volume in apneic mice. *J Appl Physiol* 2006; **101:** 454–459.
26. Zosky GR, Janosi TZ, Adamicza A, et al. The bimodal quasi-static and dynamic elastance of the murine lung. *J Appl Physiol* 2008; **105:** 685–692.
27. Kobayashi H, Hataishi R, Mitsufuji H, et al. Antiinflammatory properties of inducible nitric oxide synthase in acute hyperoxic lung injury. *Am J Respir Cell Mol Biol* 2001; **24:** 390–397.
28. Johnston CJ, Stripp BR, Piedbeouf B, et al. Inflammatory and epithelial responses in mouse strains that differ in sensitivity to hyperoxic injury. *Exp Lung Res* 1998; **24:** 189–202.
29. Achen MG, Williams RA, Minekus MP, et al. Localization of vascular endothelial growth factor-D in malignant melanoma suggests a role in tumour angiogenesis. *J Pathol* 2001; **193:** 147–154.
30. Joukov V, Pajusola K, Kaipainen A, et al. A novel vascular endothelial growth factor, VEGF-C, is a ligand for the Flt4 (VEGFR-3) and KDR (VEGFR-2) receptor tyrosine kinases. *EMBO J* 1996; **15:** 290–298.
31. Jussila L, Valtola R, Partanen TA, et al. Lymphatic endothelium and Kaposi's sarcoma spindle cells detected by antibodies against the vascular endothelial growth factor receptor-3. *Cancer Res* 1998; **58:** 1599–1604.
32. Alitalo K. The lymphatic vasculature in disease. *Nature Med* 2011; **17:** 1371–1380.
33. Dixelius J, Makinen T, Wirzenius M, et al. Ligand-induced vascular endothelial growth factor receptor-3 (VEGFR-3) heterodimerization with VEGFR-2 in primary lymphatic endothelial cells regulates tyrosine phosphorylation sites. *J Biol Chem* 2003; **278:** 40973–40979.
34. Baldwin ME, Halford MM, Roufail S, et al. Vascular endothelial growth factor d is dispensable for development of the lymphatic system. *Mol Cell Biol* 2005; **25:** 2441–2449.
35. Ikeda E, Achen MG, Breier G, et al. Hypoxia-induced transcriptional activation and increased mRNA stability of vascular endothelial growth factor in C6 glioma cells. *J Biol Chem* 1995; **270:** 19761–19766.
36. Kurihara T, Westenskow PD, Friedlander M. Hypoxia-inducible factor (HIF)/vascular endothelial growth factor (VEGF) signaling in the retina. *Adv Exp Med Biol* 2014; **801:** 275–281.